




Semi-Supervised Self-Learning-Based Lifetime Prediction for Batteries

Yunhong Che , Daniel-Ioan Stroe, *Member, IEEE*, Xiaosong Hu , *Senior Member, IEEE*, and Remus Teodorescu , *Fellow, IEEE*

Abstract—Accurate and reliable degradation and lifetime prediction for lithium-ion batteries is the main challenge for smart prognostic and health management. This article proposes a novel semi-supervised self-learning method for battery lifetime prediction. First, three health indicators (HIs) are extracted from the partial capacity-voltage curve. Second, the capacity estimation model and lifetime prediction model are built using data from three randomly selected batteries in the source domain. Then, the HIs are used to reconstruct the historical capacities to provide pseudo values for self-training of the lifetime model. Finally, the self-trained lifetime model is used to predict future degradation. The uncertainty expression is also included to provide the probabilistic prediction of future capacities. Different application scenarios are considered in the verification. The mean lifetime prediction error is less than 23 cycles with only three known checkpoints for batteries aging under different profiles. Predictions for different battery types show that the errors are less than 50 cycles with relative errors less than 4.1% for long lifespan batteries, and less than 20 cycles with relative errors less than 5.21% for short lifespan batteries. This article guides proper solutions for lifetime prediction when the labeled capacities in the real world are limited.

Index Terms—Degradation reconstruction, lifetime prediction, lithium-ion battery, probabilistic prediction, semisupervised learning.

I. INTRODUCTION

LIFETIME prediction for lithium-ion batteries attracts great research interest recently since the accurate prediction is vital for smart prognostic and health management [1], [2]. Lifetime or remaining useful life (RUL) is defined, for example, as the remaining running cycles from the current time to the

battery reaching its end of life (EOL), which is generally set as 20% capacity attenuation [3]. Methods for lifetime prediction can be divided into model-based, data-driven, and hybrid [4].

Empirical and semiempirical models, which are two categories in model-based, are widely used to fit the capacity degradation curve by some influencing factors such as temperature and state of charge. Then, the lifetime of other batteries is predicted according to the fitted curve [5]. Another model-based method is to build an electrochemical model to simulate the aging of batteries [6]. The main deficiency of model-based methods is their poor generalization ability. Data-driven method treats the battery as a “black box,” and only the data itself is studied to map the relationship between features and predictions [7]. As for battery lifetime prediction, two subcategories are widely used, i.e., the EOL prediction and degradation curve prediction. For the first one of them, the features are extracted manually [8] or automatically by deep learning [9], to fit the regression relationship with the battery lifetime. The lifetime of testing batteries can be obtained by using the regression model with the newly extracted features. However, this kind of method needs a large amount of data for feature engineering research and model training. Another problem is that only the point of EOL is predicted. However, the degradation trend should also be predicted to better understand how the battery ages and loses performance. Thus, the second kind of subcategory develops the sequence variation model of the capacity attenuation curve [10]. The rolling prediction method is then used to predict the future degradation curve until the EOL point is reached [11]. The main advantage is that future degradation is predicted which estimated the degradation rate and knee points to support early maintenance [12]. However, the main challenge is that it is difficult to correctly extrapolate the battery degradation. The main purpose of the hybrid method is to improve prediction accuracy by integrating model-based methods and data-driven methods or different kinds of data-driven methods [13], [14]. Hybrid methods rely heavily on the effectiveness of data-driven methods, where the rolling prediction method has more research and application significance than EOL point prediction. Therefore, improving the accuracy and reliability of the data-driven methods is the key challenge and basis for advanced hybrid lifetime prediction methods.

Many types of data-driven algorithms are used to fit the nonlinear degradation of the battery capacity sequence. Support vector machine [15], [16] and Gaussian process regression [1], [17] are two widely used types, but the kernel functions heavily

Manuscript received 25 April 2022; revised 24 July 2022; accepted 9 September 2022. Date of publication 15 September 2022; date of current version 4 May 2023. This work was supported in part by the Villum Foundation for Smart Battery Project No. 222860 and in part by the National Natural Science Foundation of China Grant 51875054 and Grant U1864212. Paper no. TII-22-1747. (Corresponding author: Xiaosong Hu.)

Yunhong Che, Daniel-Ioan Stroe, and Remus Teodorescu are with the Department of Energy Technology, Aalborg University, 9220 Aalborg, Denmark (e-mail: ych@energy.aau.dk; dis@energy.aau.dk; ret@energy.aau.dk).

Xiaosong Hu is with the College of Mechanical and Vehicle Engineering, Chongqing University, Chongqing 400044, China (e-mail: xiaosonghu@ieee.org).

Color versions of one or more figures in this article are available at <https://doi.org/10.1109/TII.2022.3206776>.

Digital Object Identifier 10.1109/TII.2022.3206776

influence the predictions, and it is hard to choose one kernel function that suits all capacity curves. The neural network (NN) based method is another big family that can be used to fit the capacity degradation curve [18]. It can fit any kind of nonlinear relationship via a specific combination of the weights and biases in the neurons, which makes it a feasible approach to use [19]. Popular NN for battery lifetime prediction includes basic NN, long-short term memory (LSTM) NN, convolutional NN (CNN), and gated recurrent unit NN [20], [21]. Among them, LSTM has superiority in historical information utilization, which benefits the prediction for sequence variated parameters, such as the case of the battery capacity. However, the different patterns among different batteries make it difficult to predict the degradation of other batteries that have different aging curves. Therefore, transfer learning (TL) is proposed to improve the lifetime prediction accuracy [22]. Another advantage of NN-based prediction is that the model-based TL strategy can be conveniently integrated into the retraining process, which helps improve the accuracy of prediction and model generalization ability. The main purpose of TL is to use the knowledge gained from the previously trained model while integrating the testing information by only retraining some chosen parameters, which accelerates the training process and improves the model accuracy [23]. However, the main problem for capacity degradation curve prediction is that there are not enough continuously changed capacity values for model retraining in real applications. Therefore, the capacity estimation model could be used to estimate the capacity with partial process data [24]. Another limitation of published papers is that the TL is only implemented to predict the degradation of the same battery types under similar working conditions.

This article proposes a novel method for battery capacity degradation prediction based on semi-supervised self-learning (SSSL) strategy, which is realized by historical degradation reconstruction and lifetime model self-training based on a few discontinuous checkpoints. The main contributions are summarized as follows.

- 1) A self-training process is proposed to improve the lifetime prediction model using pseudocapacities.
- 2) Only a few discontinuous checkpoints are needed for continuous capacity degradations prediction.
- 3) The HIs are extracted from the partial curves to reconstruct the historical capacities.
- 4) The proposed SSSL prediction method has a great generalization to predict the future degradation trend of different battery types or/and different aging conditions with uncertainties.

The remainder of the article is structured as follows; the datasets used in this article are introduced in Section II. Then, the proposed battery historical capacity curve reconstruction and lifetime prediction method are described in Section III. Followed that, the results are presented and discussed in Section IV. Finally, Section V concludes this article.

II. DATA DESCRIPTION

The datasets used in this article contain both public data from [25], [26] and experimental data generated by the authors. The

TABLE I
DETAILED INFORMATION OF THE DATASETS

Battery data set	Geometry	Chemistry	Nominal capacity
SD	Cylindrical	LFP/C	1.1 Ah
TD1	Cylindrical	LFP/C	1.1 Ah
TD2	Prismatic	LFP/C	110 Ah
TD3	Prismatic	LFP/C	100 Ah

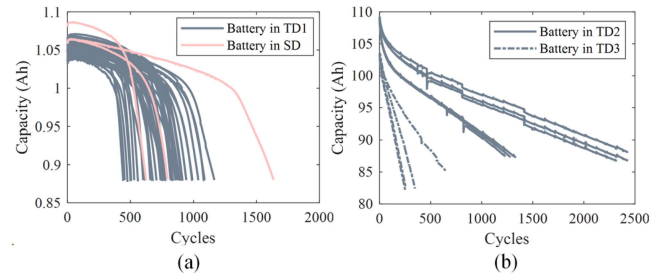


Fig. 1. Capacity fade curve of batteries in (a) SD and TD1, and (b) TD2 and TD3.

detailed information is given in Table I. The datasets are divided into the source domain (SD), which contains three randomly selected batteries from [24] with different life ranges, and the target domain (TD). In the TD, three datasets are included. One is from the public dataset presented in [26] that has the same battery types as those in SD but has fast charging protocols (named TD1). The capacity fade curves of the batteries in the SD and TD1 are shown in Fig. 1(a). They have similar degradation patterns due to the same battery chemistry and format with large but similar current loadings. However, Fig. 1(a) still shows that different aging rates exist among different battery cells. The reason could be that the current rates of the loading profiles have differences, and manufactural inconsistency exists among different battery cells [27].

Another two experimental datasets are also included in the TD. The first one has a nominal capacity of 110 Ah (named TD2), and the second has a nominal capacity of 100 Ah (named TD3). They are from different commercial companies and have large differences in the life ranges as shown in Fig. 1(b). These two datasets have different battery formats and working profiles from those in SD and TD1 although the chemistries are the same. The batteries in TD2 and TD3 are prismatic while those in SD and TD1 are cylindrical. The loading current rates for TD2 and TD3 are much less than those for SD and TD1, and the charging modes are also different. These differences make the batteries in TD2 and TD3 have quite different degradation patterns to those in SD and TD1. The shapes of the degradation curves in TD2 and TD3 are different from those in SD and TD1. In TD2 and TD3, batteries show a fast degradation rate in the early stage while a slow and nearly linear degradation rate exists in the later stage, which is opposite to that in SD and TD1. These ten batteries (cells 1–6 in TD2, and cells 7–10 in TD3) are aged under constant current constant voltage (CCCV) charging and CC discharging. The detailed setting information of the experiment for each cell is given in Table II. Cells 1–7 are

TABLE II
EXPERIMENT OF BATTERIES IN TD2 AND TD3

Battery cell	Charge-discharge rate	Environment temperature	Capacity range	Cycles
Cell 1	1C-1C	55 °C	87.32-109.15	1282
Cell 2	1C-1C	55 °C	87.46-109.30	1231
Cell 3	1C-1C	55 °C	87.26-109.06	1334
Cell 4	1C-1C	35 °C	88.13-109.07	2431
Cell 5	1C-1C	35 °C	86.83-108.42	2313
Cell 6	1C-1C	35 °C	86.81-107.97	2431
Cell 7	1C-1C	25 °C	82.45-103.04	346
Cell 8	0.5C-0.5C	35 °C	85.23-103.08	645
Cell 9	0.5C-0.5C	55 °C	82.28-102.81	250
Cell 10	0.5C-0.5C	55 °C	82.77-103.44	254

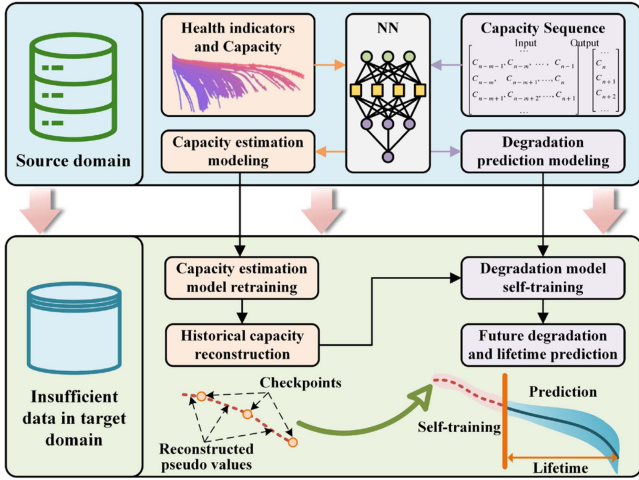


Fig. 2. Overall framework for SSSL-based battery lifetime prediction.

aged with a current rate of 1C, and cells 8–10 are aged at 0.5C. The temperature is 55 °C for cells 1–3 and cells 9 and 10, 35 °C for cells 4–6 and cell 8, while 25 °C for cell 5. As one can observe, the batteries in TD2 and TD3 are aged under different conditions, which causes them to have different degradation patterns and cycle lives. Therefore, the datasets used in this article contain scenarios for predictions under different working conditions and different battery formats/geometry.

III. PREDICTION METHOD

The overall framework of the SSSL-based battery lifetime prediction is shown in Fig. 2. The datasets are divided into a SD and a TD with insufficient labeled data. Specifically, two NNs-based models will be trained in the SD, one for the HIs-based capacity estimation model and the other for the capacity degradation model. These two base models are trained offline using ample data to make sure the models are well trained. Then, in the TD, which has only sparse and limited labeled data, the capacity estimation model is first retrained to reconstruct the historical degradation curve of capacities considering only a limited number of checkpoints. The historical capacities are reconstructed by the capacity estimation model using the proposed HIs. Following that, the degradation model is self-trained using the estimated pseudo capacity values. Here, the main

difference between training and self-training is whether real labels or pseudolabels are used. The retraining and self-training processes are conducted online with the available checkpoints. It could be trained fast since only limited data are used, and the base model helps accelerate the convergence speed. Therefore, the model construction process contains offline calibration and online adjustment to improve the estimation and prediction accuracy as well as the model generalization. Finally, the future degradation trajectory is predicted until reaches the EOL for the battery lifetime prediction. In the degradation prediction model, the predicted capacities are used for the iterative prediction. The advantages of the proposed SSSL-based method compared to the conventional LSTM-based method mainly exist in the following three aspects.

- 1) The sparse and limited labeled checkpoints are used to retrain the capacity estimation model, while the unlabeled historical data could be well reconstructed.
- 2) The pseudovalues of the estimated capacities are utilized for the self-training of the degradation prediction model to improve the accuracy of the future degradation prediction. Therefore, both the process data (voltage, current, and time) and labeled capacities are well used to improve the accuracy of the prediction models.
- 3) The probabilistic regression is integrated to provide the confidence interval (CI) of the predicted capacity curve. In the following subsections, the detailed modeling and training process will be described.

A. Capacity Reconstruction

The main process for pseudo capacity reconstruction includes HIs extraction, capacity estimation model training, and retraining with a limited number of checkpoints.

1) *Health Indicators Extraction*: The incomplete charging and discharging in most real conditions require indirect capacity estimation to support battery management, which can be realized by the feature-based data-driven method. It is known that ample aging information is hidden behind the battery capacity-voltage (Q - V) curves, which show regular changes along with aging [19]. The partial Q - V is used for HIs extraction in this article. The volage sequence is divided equally into 1000 segments from the lowest voltage to the highest voltage. Then, the voltage sequence from 2.85 to 3.25 V is selected in this article. The voltage sequence for each cycle is denoted as $[V_m, V_{m+1}, \dots, V_{n-1}, V_n]$. The charged capacity (Q) value between each voltage segment is calculated to form the Q sequence, which is denoted as $[Q_m, Q_{m+1}, \dots, Q_{n-1}, Q_n]$. Finally, three HIs are extracted from the Q sequence. Here, the three HIs including standard deviation, Shannon entropy, and the first principal component are calculated. The standard deviation and Shannon entropy are calculated by the corresponding value of the Q sequence from each cycle. The first principal component is extracted by dimension reduction of the Q matrix, which is formed by the Q sequence at different cycles. It is known that the Q - V curve varies regularly with aging. The standard deviation can describe the degree of this variation. The Shannon entropy is a good indicator to reflect the amount of information contained in the sequence.

TABLE III
MEAN CORRELATION COEFFICIENT FOR THE THREE HIS

Data sets	Standard deviation	Shannon entropy	First principal component
SD	0.9681	0.9702	0.9622
TD1	0.9578	0.9609	0.9502
TD2	0.9711	0.9910	0.9659
TD3	0.9774	0.9794	0.9654

The principal component analysis is used to describe the internal relationships of the sequence by several principal components, where the first component describes the main degradation trend of the Q sequence. Therefore, these three HIs are good indicators to describe the health status of batteries indirectly.

To evaluate the effectiveness of the three HIs, Pearson correlation coefficients between the HIs and battery capacities are calculated. The mean correlation coefficient values for the four datasets are given in Table III. The results show that the mean correlation coefficients for all the three HIs regarding all the four datasets is larger than 0.95, which indicates the HIs have high correlations with battery capacities. Therefore, the three HIs could be used to reconstruct the historical capacities for the pseudo values preparation in the next subsection.

2) Pseudocapacity Reconstruction: According to the extracted HIs from the partial curve, the pseudo capacities in the historical degradation process can be reconstructed with a limited number of checkpoints for model retraining. First, the NN-based capacity estimation model is pretrained using the data from the SD, where the inputs are the HIs extracted above and the output is battery capacity for each cycle. The NN is constructed by an LSTM layer with the activation function of *relu* and a dense layer. The basic calculation for the LSTM is performed as presented in [28]

$$f(t) = \sigma(w_{f1}x(t) + w_{f2}h(t-1) + b_f) \quad (1)$$

$$i(t) = \sigma(w_{i1}x(t) + w_{i2}h(t-1) + b_i) \quad (2)$$

$$\tilde{S}(t) = \tanh(w_{c1}x(t) + w_{c2}h(t-1) + b_c) \quad (3)$$

$$S(t) = f(t) \odot S(t-1) + i(t) \odot \tilde{S}(t) \quad (4)$$

$$o(t) = \sigma(w_{o1}x(t) + w_{o2}h(t-1) + b_o) \quad (5)$$

$$h(t) = o(t) \odot \tanh(S(t)) \quad (6)$$

where $x(t)$ and $h(t)$ are the input and output, respectively, $S(t)$ is the state information, $f(t)$, $i(t)$, and $o(t)$ are the information updated by the forget gate, input gate, and output gate respectively, w and b are the weights and biases, respectively, σ and \tanh are the activation functions.

Then, for the historical capacity reconstruction of the tested batteries, only a few checkpoints with labeled data are needed for the retraining of the last dense layer. The checkpoints here could be obtained in the real world during the regular maintenance process, which makes it realistic. Finally, the retrained model is used to reconstruct the historical capacity between the checkpoints. The reconstructed capacities are used as pseudo values for the self-training process of the lifetime model in the following section.

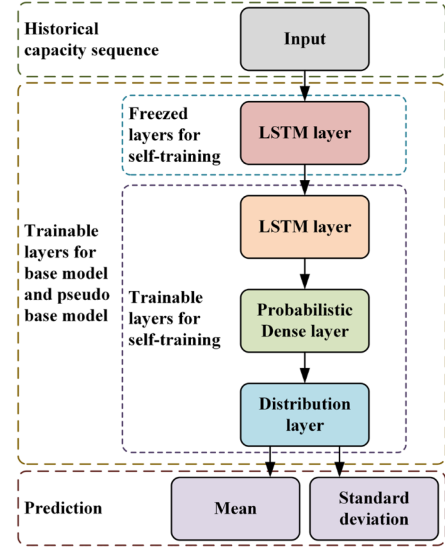


Fig. 3. Framework and training process of the proposed lifetime model.

B. Lifetime Prediction

The extrapolation method is adopted to predict the future capacity with uncertainty based on transferable NN, which is proposed in this section. The proposed framework of the NN is shown in Fig. 3. The basic training, transferred basic training, and self-training processes are described in the following section.

1) Lifetime Modeling: For sequence-based capacity prediction, the capacities are firstly reconstructed to form the inputs and output as

$$[C_{i-m}, C_{i-m+1}, \dots, C_{i-1}, C_i] \quad (7)$$

$$[C_{i+1}, C_{i+2}, \dots, C_{i+n}] \quad (8)$$

where C_i is the capacity of i th cycle, m and n represent the input length and predicted length, respectively. In this article, m is set as 9 and n is set as 1, which means the length of input and output are 10 and 1, respectively.

Then, the NN framework shown in Fig. 3 is used for the model training. Here, two LSTM layers are first added. Then, a probabilistic dense layer is considered. The basic function for the probabilistic dense layer is the same as the dense layer, while the weights and biases are set as distributions instead of specific values. The last layer is a DistributionLambda (Distribution) layer to output the predicted distribution. The negative log-likelihood loss function is used for the loss minimization [29]

$$\text{loss}(z, y) = -y.\log_prob(z) \quad (9)$$

where y and z are the predicted distribution and real target respectively, $y.\log_prob(z)$ means to get the logarithmic probability (logprob) of one experiment sample (z) under a specific distribution (y). The lifetime model is first trained using the data of the three batteries in the SD. Then, the SSSL process is adopted to update the model for the lifetime prediction of testing batteries in TD, which is introduced in the following section.

2) Self-Training for Prediction: The degradation curves of the battery in SD are different from those in TDs. If the trained lifetime model by SD is directly used to predict the future degradation of batteries in TDs, the predictions would separate from real values. Therefore, the SSSL is proposed in this article to improve the adaptation of the predictions under different applications.

The first scenario is to predict the lifetime of batteries that have the same battery types, but different working conditions compared with the batteries in SD. Here, the first LSTM layer is frozen after being trained by the data of batteries in SD to retain the general degradation characteristics of this type of battery. The second LSTM, probabilistic Dense layer, and Distribution layer are set trainable to learn specific information about each testing battery. The reconstructed historical capacity curve of the testing battery is used for self-training to improve the lifetime model. Finally, the future degradation curve is predicted by extrapolating the predicted values.

The second scenario is to predict the lifetime of batteries that have different battery types to the batteries in SD. In this condition, one battery in TD is selected to reconstruct the whole degradation curve with seven checkpoints (1st, 10% cycle, 30% cycle, 50% cycle, 70% cycle, 90% cycle, and the last cycle). Then, the whole lifetime model is retrained to adapt to the degradation patterns of this kind of battery using the pseudo capacities. Here, the lifetime model trained by batteries in SD provides the initial values of parameters for training. After the model is retrained, the same process of the self-training in the previous paragraph is used for the degradation prediction of other batteries in TD. In this scenario, two self-training processes are used to improve the lifetime model for degradation prediction.

IV. RESULTS AND DISCUSSION

In this section, the two application scenarios discussed above are used for verification. The evaluation is discussed by analyzing both the lifetime prediction error and the accuracy of the future predicted capacity curve compared to the real curve. The prediction framework proposed in this article is built based on Keras and TensorFlow Probability.

A. Prediction for Same Battery Types With Different Profiles

The results of the prediction for batteries that have the same battery types but different working conditions are discussed in this section. Although, the batteries with same battery types have similar degradation patterns, the degradation rates and shapes still show differences, which have been shown in Fig. 1(a). Here the three batteries in SD are used for base model training. Then, the SSSL is implemented in TD1 to demonstrate the effectiveness of the lifetime prediction.

The lifetime predicted errors (different cycles between the predicted RUL and real RUL from start points), root-mean-square error (RMSE), and mean absolute error (MAE) of the whole predicted capacities are shown in Fig. 4. The RMSE and MAE are calculated by the whole predicted capacities, which include the historical reconstructed part and future predicted

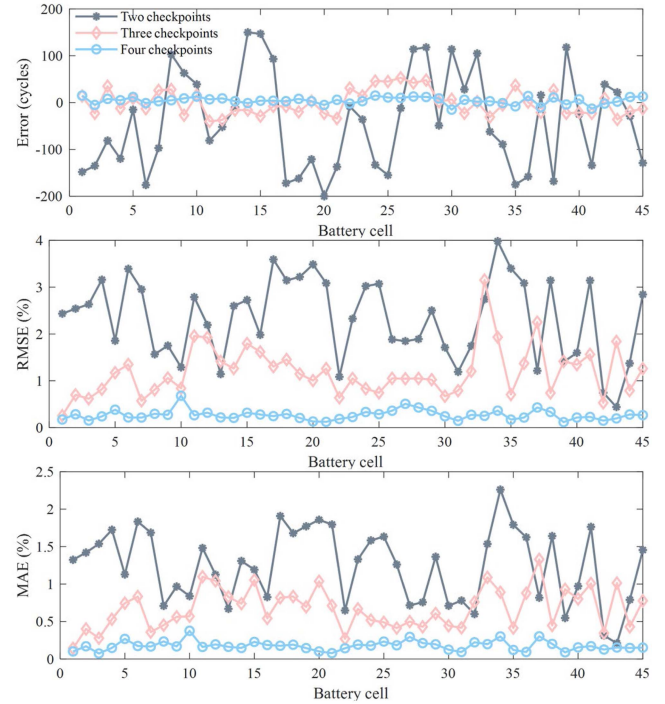


Fig. 4. Predicted lifetime error, capacity RMSE and MAE of all the 45 batteries in TD1.

TABLE IV
PREDICTED ERRORS OF TD1

Checkpoints	Mean absolute error of lifetime	Mean RMSE of capacities	Mean MAE of capacities
2	96.40 cycles	2.33%	1.24%
3	22.68 cycles	1.19%	0.67%
4	7.27 cycles	0.27%	0.18%

part together. The mean errors of these 45 battery cells are given in Table IV. The checkpoints here mean some known data of the testing battery cell, which are the data at 10%, 30%, 50%, and 90% of the whole cycle life. Two checkpoints mean the first two checkpoints are included, three checkpoints include the first three, and all four checkpoints are included in the last case. Note that it is hard and unrealistic to obtain sufficient labeled data for model construction in practical applications, while sparsely labeled data could be obtained (e.g., in regular maintenance). Therefore, the sparsely labeled checkpoints are used for the retraining and self-training process in this article to demonstrate the improvement of the proposed SSSL method in the battery degradation curve and lifetime prediction. Fig. 4 shows that the prediction errors reduce significantly with the increase of checkpoints used for self-training. When three checkpoints are available, the absolute lifetime prediction errors vary within 50 cycles. All the RMSEs are less than 3.15% and all MAEs are less than 1.4%. Although three checkpoints are used, a very few capacities range is included since the capacity degrades very slowly in the early stages. Therefore, the results have low prediction errors and good generalization for all the cells. When one more checkpoint is obtained during the later battery usage,

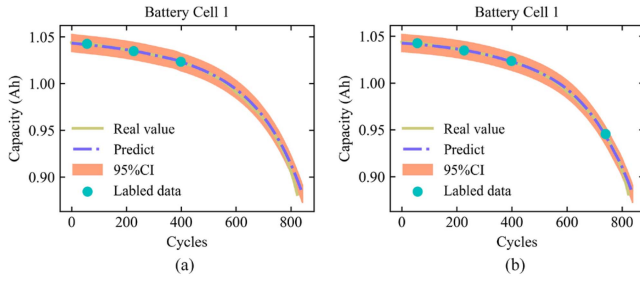


Fig. 5. Prediction results for battery cell 1 using (a) three checkpoints and (b) four checkpoints.

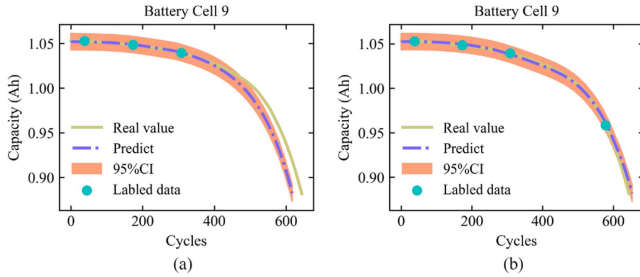


Fig. 6. Prediction results for battery cell 9 using (a) three checkpoints and (b) four checkpoints.

which is in the faster changing stage, the predicted errors decline rapidly. All the absolute predicted lifetime errors are less than 15 cycles. All the RMSEs and MAEs are less than 0.68% and 0.38% respectively.

The mean errors of the lifetime prediction and future capacity prediction are given in Table IV. It shows that when only two checkpoints in early stages are used, the mean lifetime prediction error is 96.4 cycles, which is reduced sharply to 22.68 when the third checkpoint is available. The mean RMSE and MAE currently are only 1.19% and 0.67%, which means the predicted capacities are close to the real capacities. When one more checkpoint that is in the fast-degrading stage is obtained, the mean lifetime prediction error is only 7.27 cycles, and the mean RMSE and MAE are only 0.27% and 0.18%, respectively. Therefore, the statistical results of all the batteries in TD1 illustrate that the proposed method predicts the future capacity degradation satisfactorily and has good generalization for different working conditions and lifetime ranges.

The prediction results of three batteries in TD1 are shown in Figs. 5–7, which are the results of cells 1, 9, and 3 in TD1 respectively. In each figure, subfigure (a) represents the results predicted by three available checkpoints and subfigure (b) is the results obtained by four available checkpoints. The selection of these three battery cells is performed according to the prediction results when three checkpoints are obtained. Fig. 5(a) is representative of the case when the predicted lifetime is close to the real lifetime considering three checkpoints. Fig. 6(a) is representative of the case when the predicted lifetime is underestimated, while Fig. 7(a) is representative of the case when the predicted lifetime is overestimated, both cases considering three checkpoints. Fig. 5(a) shows that although the lifetime prediction is accurate, the future capacity continues to become more accurate

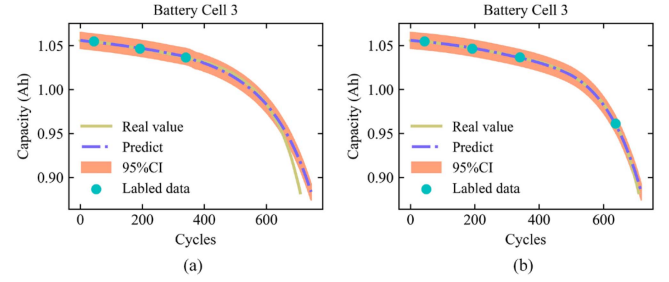


Fig. 7. Prediction results for battery cell 3 using (a) three checkpoints and (b) four checkpoints.

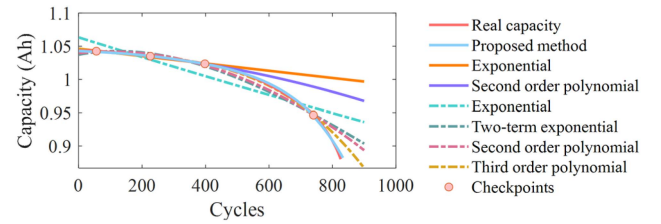


Fig. 8. Comparison between the proposed method and curve fitting methods.

with one more checkpoint, as illustrated in Fig. 5(b). The RMSE and MAE of the predicted capacity curve are reduced to 0.17% and 0.10% from 0.26% and 0.14% respectively. In Fig. 6(a), the predicted lifetime is shorter than the real lifetime, which has an error of 27 cycles. But, the predicted future capacities still show similar degradation patterns to the real curve. The predicted RMSE and MAE of the capacity curve are 1.06% and 0.56%, respectively. However, when one more checkpoint that lies in the fast-changing process is available, the predicted curve converges to the real curve better. The predicted lifetime error is reduced to 9 cycles, and the RMSE and MAE of the predicted capacity curve are reduced to 0.27% and 0.17%, respectively. As for battery cell 3, in Fig. 7(a), the predicted lifetime is longer than the real value with an error of 35 cycles. Similarly, the future predicted capacity curve is still close to the real values with the RMSE and MAE at only 0.62% and 0.15%, respectively. When the fourth checkpoint is obtained as shown in Fig. 7(b), the prediction becomes better, with a lifetime prediction error only of eight cycles. The RMSE and MAE of the whole predicted capacity curve are only 0.15% and 0.07% currently. The 95% CI covers the real values to show the reliability of the predicted values.

From the results presented above, the proposed method is proved to have satisfactory performance to reconstruct the historical degradation curve and predict the future trajectory with only a few checkpoints. To further evaluate the proposed prediction framework, the comparison with curve fitting methods with the known checkpoints is presented in Fig. 8. The results are obtained from battery cell 1. The solid lines represent the real value and the predictions obtained with three checkpoints. Since the unknown parameters of the empirical model should be less than the known checkpoints, the exponential and second-order polynomial functions are used. The results indicate that the curve

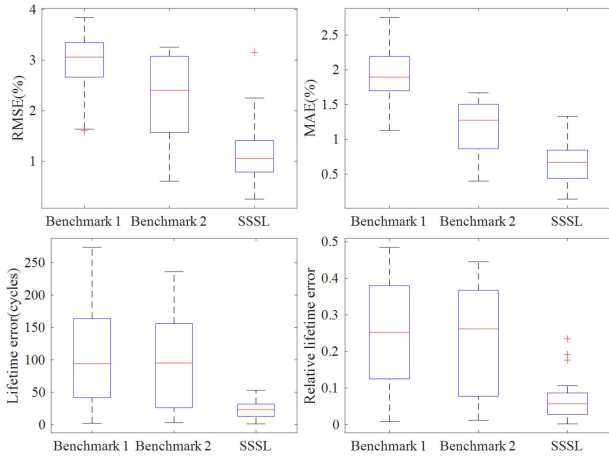


Fig. 9. Comparisons between the proposed method and two benchmarks.

fitting methods failed to predict the real degradation curve with such limited checkpoints. When four checkpoints are obtained, the fitted curves, represented by dot-dash lines, still have large deviations from the real curve. The most similar prediction obtained by the third-order polynomial function still has an error of 52 cycles, which is much larger than the prediction of the proposed method with only three checkpoints. Therefore, the comparison indicates that the proposed method has higher accuracy for battery future capacity and lifetime prediction with limited known labeled data.

To evaluate the improvement of the proposed SSSL for battery lifetime prediction, two benchmarks are used for comparison. The two benchmarks adopt the same model structure for capacity estimation and degradation trajectory prediction. The differences are whether the capacity estimation model is retrained by the sparse checkpoints and the degradation prediction model is self-trained by the estimated pseudo capacities. Benchmark 1 refers to the results obtained by the base capacity estimation model to estimate the capacity and degradation model to predict the future capacity fade using the estimated capacity without any retraining or self-training process. Benchmark 2 refers to that the capacity estimation model is retrained by the sparse checkpoints and the capacity is estimated by the retrained model. Then, the degradation curve is predicted by the estimated capacities using the base degradation prediction model. While the proposed SSSL method conducted self-training to improve the degradation prediction model using the estimated capacities and then predict the future degradation curves. Therefore, it means that benchmark 1 is without any retraining or self-training, benchmark 2 has retraining but no self-training, and the proposed SSSL has both retraining and self-training. It could be seen that benchmark 1 is the basic LSTM method for battery lifetime prediction, and benchmark 2 is the basic LSTM with TL for battery lifetime prediction.

Three checkpoints are used in this comparison. The boxplot for the capacity and lifetime prediction errors is shown in Fig. 9. It shows that the capacity estimation errors are reduced when the capacity estimation model is retrained in benchmark 2 compared

TABLE V
COMPARATIVE RESULTS BETWEEN TWO BENCHMARKS AND THE SSSL

Index	Benchmark 1	Benchmark 2	SSSL
RMSE (%)	2.93%	2.27%	1.19%
MAE (%)	1.92%	1.18%	0.67%
Lifetime error (cycles)	106.42	81.93	22.68
Relative lifetime error (%)	25.09%	20.54%	6.37%
Computational time (s)	21.28	28.06	38.49

to that in benchmark 1. However, all errors are still much larger than those in the proposed method, because the future degradation prediction (in benchmarks 1 and 2) is poorer than for the proposed method. The lifetime prediction of benchmark 2 improves slightly compared to benchmark 1. The reason could be that although the degradation curve is poorly predicted, the final errors of the predicted lifetime may not show much difference. But, all the capacity and lifetime prediction errors are reduced significantly by the proposed SSSL method, which means the capacity estimation model retraining and degradation model self-training helps improving the prediction accuracy for the whole degradation curve.

The absolute values of the mean RMSE and MAE for the predicted capacities, the mean error and mean relative error for the predicted lifetime, and the computational time of the whole prediction process for the 45 batteries in TD1 are given in Table V. The results show the improvement trend from benchmark 1 (which can be seen as the traditional LSTM method) to benchmark 2 (which can be seen as LSTM with TL), and to the proposed method. The mean RMSE and MAE of the proposed method are reduced by 59.39% and 65.10% compared to the traditional LSTM method (benchmark 1). The lifetime prediction error and relative lifetime prediction error are reduced by 78.69% and 74.61% compared to the traditional LSTM method. The computational time is calculated by the time for the whole capacity estimation model retraining, degradation prediction model self-training, historical capacity reconstruction, and future capacity prediction. The mean time for the calculation of the 45 battery cells is the final computational time in Table V. The results show that the further retraining and self-training process does not require too much additional computation, which just increases by about 17s (less than 81%). Considering the satisfactory accuracy improvement and the acceptable computational burden increment, the proposed method shows great improvement in the battery degradation and lifetime predictions with sparse and limited labeled checkpoints.

B. Predictions for Different Battery Types

The predictions presented in the above section represent the applications for the same battery type with different aging profiles. In real applications, the prediction for different battery types that have different degradation patterns is also widely required. Therefore, the prediction under this applicable scenario using the proposed method is evaluated in this section. In this application, since the degradation patterns are quite different from the batteries in SD, one battery with seven checkpoints is first used to reconstruct the capacity curve for lifetime model

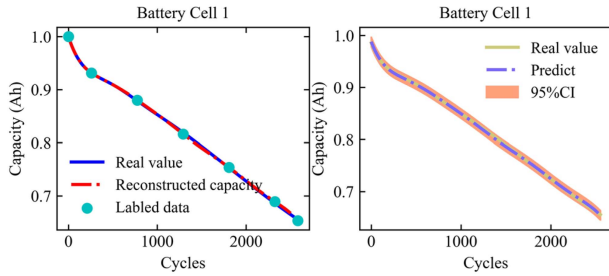


Fig. 10. Capacity reconstruction and lifetime model retraining.

self-training. Then, the self-trained model is further improved following the process in the above section to predict the future capacity and lifetime of this new type but different aging characteristic batteries.

1) *Predictions for Batteries in TD2*: The predictions for batteries in TD2 are presented and evaluated in this section. First, battery cell 1 in TD2 is used to retrain all the networks with seven checkpoints to learn the specific characteristics of this kind of battery type. The capacity reconstruction and lifetime prediction model training results are shown in Fig. 10. The left subfigure is the capacity reconstruction results and the right subfigure is the lifetime model retrained results. The obtained results show that the capacity fade curve of one battery can be well reconstructed with only seven checkpoints. The reason is that the HIs used for capacity estimation have high Pearson correlation coefficients with battery capacities for all four datasets. The model could be updated fast and converged quickly with only a few checkpoints. The whole capacity degradation curve could be well reconstructed to provide the pseudo values for lifetime model retraining. Then, the estimated pseudo capacities are used to retrain the whole degradation prediction model. The lifetime model trained by the pseudo values also covers the real degradation curve correctly with small 95% CIs. Although only a few checkpoints are used, the specific degradation pattern of the new battery-type under new aging profiles could be learned using the semisupervised learning strategy. Therefore, the retrained model can be used in the same way as in the former section to predict the lifetime of other batteries of the same battery types but with different degradation curves.

The lifetime prediction results for battery cells–6 are shown in Fig. 11. Here, only three checkpoints at the early stage (100th, 200th, and 300th cycle) are used. The results show that the predictions for these five battery cells are accurate despite different life ranges. The future capacities follow the real values correctly and the 95% CIs converge the real capacity curve successfully, indicating the effectiveness of the proposed method to predict the lifetime of different battery types and different aging profiles. To evaluate the influence of selection of the first retrained battery, cell 6 is firstly used to retrain the whole NN and to predict the lifetime of cell 1 by continued self-training using the three early checkpoints. The results show that the prediction is also accurate and reliable. Therefore, the proposed method has good generalization ability.

The numerical results of the lifetime predictions for TD2 are given in Table VI, and the errors of the future predicted capacity

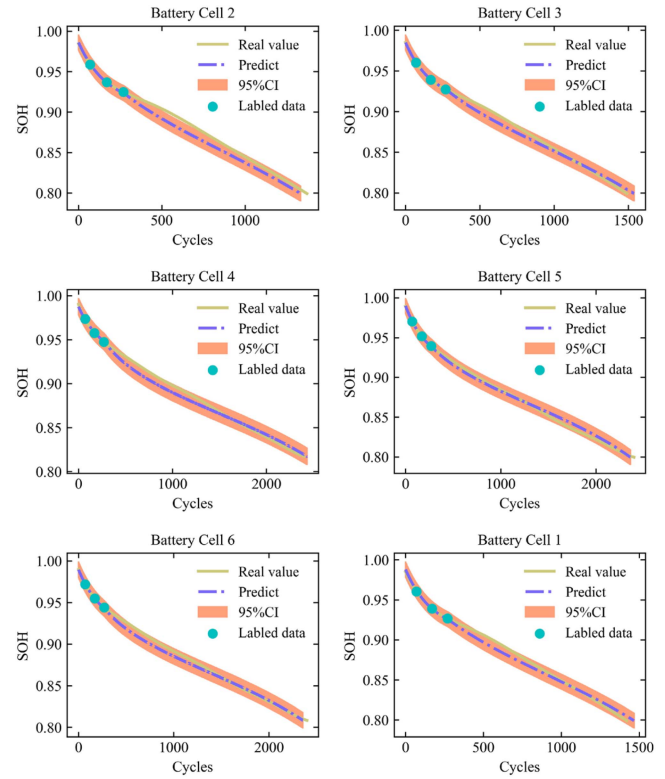


Fig. 11. Lifetime prediction results for batteries in TD2.

TABLE VI
LIFETIME PREDICTED ERRORS OF TD2

Battery cell	Real lifetime	Predicted lifetime	Absolute error	Relative error
Cell 1	982	1029	47 cycles	4.08%
Cell 2	931	893	-38 cycles	-3.44%
Cell 3	1034	1082	48 cycles	3.93%
Cell 4	2131	2164	33 cycles	1.55%
Cell 5	2013	1975	-38 cycles	1.78%
Cell 6	2131	2088	-43 cycles	2.02%

TABLE VII
CAPACITY PREDICTED ERRORS OF TD2

Battery cell	RMSE of capacities	MAE of capacities
Cell 1	0.51%	0.41%
Cell 2	0.81%	0.70%
Cell 3	0.53%	0.41%
Cell 4	0.54%	0.45%
Cell 5	0.36%	0.30%
Cell 6	0.44%	0.34%

curve are given in Table VII. The remaining lifetime of the batteries aged under 55 °C is about 1000 cycles while that of the batteries aging under 35 °C is more than 2000 cycles. The results show that the predicted lifetime errors are less than 50 cycles for all these six batteries. Therefore, the relative errors are less than 4.1% for the batteries aged under 55 °C with about 1000 cycles remaining. Furthermore, the relative errors are less than 2.1% for the batteries aged under 35 °C with more than 2000 cycles remaining. The predicted errors are low enough in this case for

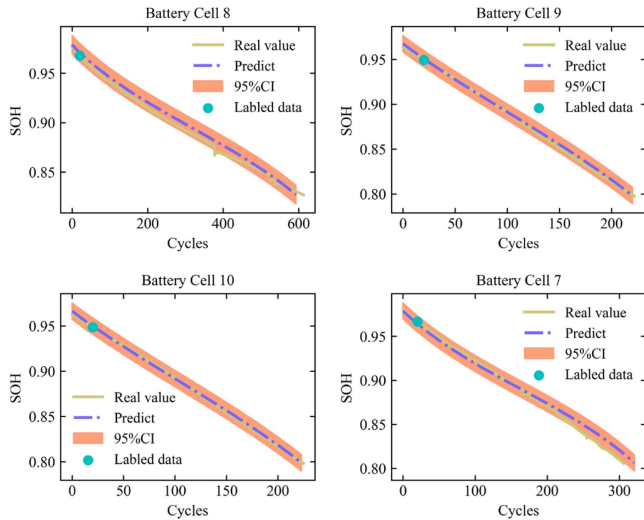


Fig. 12. Lifetime prediction results for batteries in TD3.

TABLE VIII
LIFETIME PREDICTED ERRORS OF TD3

Battery cell	Real lifetime	Predicted lifetime	Absolute error	Relative error
Cell 7	296	311	15 cycles	5.21%
Cell 8	595	575	-20 cycles	-3.36%
Cell 9	200	198	-2 cycles	-0.98%
Cell 10	204	202	-2 cycles	-0.97%

early lifetime prediction. The errors for the predicted capacity curve are small for all the batteries. The RMSEs are less than 0.81% and the MAEs are less than 0.70%, which indicates the accuracy and reliability of the future capacity curve prediction. Therefore, from the results presented above, we can conclude that the proposed method can predict the future capacity fade curve and lifetime prediction with only 7 checkpoints for first retraining and three early checkpoints for self-training even though the testing batteries have different battery types and different aging patterns with the known batteries in SD.

2) Predictions for Batteries in TD3: Finally, the predictions for the third testing battery dataset (TD3) are presented and evaluated in this section. The prediction method for this dataset is the same as that for TD2. The battery cell 7 is first used for the retraining of the whole NN, and then used to predict the lifetime of cells-10. For the prediction of cell 7, the information of cell 10 is first used.

The prediction results for these four batteries are shown in Fig. 12. Since the life ranges of this type of battery are short and the window size is set as 30, the early degradation characteristics are not shown in the figures. But, the whole degradation curves of TD3 shown in Fig. 1(b) clearly illustrate the early degradations. Only one checkpoint (50th cycle) is used for historical capacity reconstruction and lifetime model self-training in this case. The prediction results shown in Fig. 12 indicate that the predicted degradation curves are close to the real curves, with CIs that converge the real values satisfactorily.

TABLE IX
CAPACITY PREDICTED ERRORS OF TD3

Battery cell	RMSE of capacities	MAE of capacities
Cell 7	0.56%	0.43%
Cell 8	0.53%	0.48%
Cell 9	0.23%	0.19%
Cell 10	0.16%	0.14%

The numerical results are given in Tables VIII and IX to show the accuracy of the predicted lifetime and capacity curve. Results show that the lifetime prediction errors are less than 20 cycles, and the relative errors are less than 5.3% even if the denominator is less than 300 cycles. The errors for the whole predicted capacity errors are also small. The RMSEs are no more than 0.56% while the MAEs are no more than 0.48%, indicating accurate prediction results. The above prediction results verify that the proposed method could support early lifetime predictions with very few checkpoints.

V. CONCLUSION

Degradation curve prediction and lifetime prediction are significant, but challenging tasks for smart battery management. This article proposed a novel SSSL-based prediction framework. First, three randomly selected batteries from a public dataset were used to train the base models for battery capacity reconstruction and lifetime prediction. Three HIs from the partial curve were extracted for the capacity reconstruction. Then, the self-training process was proposed to improve the model by taking advantage of the pseudovalues. Moreover, only a few labeled checkpoints were needed, which conforms to the real applications that limited labeled but abundant unlabeled data were available. Finally, the proposed prediction framework was evaluated under different application scenarios, where different battery types and/or different aging profiles are considered. The experimental results show that when the base model was directly used for the predictions of the same battery type, but different aging profiles, the mean lifetime errors were less than 23 cycles using only three checkpoints, and the errors are reduced to less than eight cycles when one more checkpoint, corresponding to the fast-changing stage is used. When the framework was applied for lifetime prediction of different battery types, one cell with seven checkpoints was used to retrain the base models first, and then used for other battery predictions. Results show that the predicted errors are less than 50 cycles, and the relative errors are less than 4.1% for TD2 that have a lifespan of over 2000 cycles with only three labeled checkpoints in the early 300 cycles. The predicted errors for TD3 that have a short life span are no more than 20 cycles with relative errors of no more than 5.21% with only one checkpoint from the 50th cycle. Therefore, the proposed method can achieve early future degradation curve prediction with satisfactory accuracy and reliability. It can be seen that the proposed SSSL-based battery degradation prediction method helps improve the accuracy by capacity estimation model retraining and degradation prediction model self-learning. It should be noted that other HIs proposed

in other state-of-the-art works could also be used in the capacity estimation model to explore the application scopes. In future work, the temperature information would be considered to improve the prediction accuracy under degradations with variable temperature scenarios. The degradation and lifetime prediction for batteries with different chemistries will also be an interesting and significant research focus.

REFERENCES

- [1] K. Liu, Y. Li, X. Hu, M. Lucu, and W. D. Widanage, "Gaussian process regression with automatic relevance determination kernel for calendar aging prediction of Lithium-Ion batteries," *IEEE Trans. Ind. Inform.*, vol. 16, no. 6, pp. 3767–3777, Jun. 2020, doi: [10.1109/TII.2019.2941747](https://doi.org/10.1109/TII.2019.2941747).
- [2] X. Hu, Z. Deng, X. Lin, Y. Xie, and R. Teodorescu, "Research directions for next-generation battery management solutions in automotive applications," *Renew. Sustain. Energy Rev.*, vol. 152, 2021, Art. no. 111695.
- [3] Z. Zhang, Y. Jeong, J. Jang, and C. G. Lee, "A pattern-driven stochastic degradation model for the prediction of remaining useful life of rechargeable batteries," *IEEE Trans. Ind. Inform.*, early access, doi: [10.1109/TII.2022.3155597](https://doi.org/10.1109/TII.2022.3155597).
- [4] X. Hu, L. Xu, X. Lin, and M. Pecht, "Battery lifetime prognostics," *Joule*, vol. 4, no. 2, pp. 310–346, 2020, doi: [10.1016/j.joule.2019.11.018](https://doi.org/10.1016/j.joule.2019.11.018).
- [5] Y. Li et al., "Data-driven health estimation and lifetime prediction of Lithium-Ion batteries: A review," *Renew. Sustain. Energy Rev.*, vol. 113, 2019, Art. no. 109254.
- [6] I. Baghdadi, O. Briat, J. Y. Deléage, P. Gyan, and J. M. Vinassa, "Lithium battery aging model based on Dakin's degradation approach," *J. Power Sources*, vol. 325, pp. 273–285, 2016.
- [7] X. Hu, Y. Che, X. Lin, and Z. Deng, "Health prognosis for electric vehicle battery packs: A data-driven approach," *IEEE/ASME Trans. Mechatronics*, vol. 25, no. 6, pp. 2622–2632, Dec. 2020.
- [8] P. M. Attia, K. A. Severson, and J. D. Witmer, "Statistical learning for accurate and interpretable battery lifetime prediction," *J. Electrochem. Soc.*, vol. 168, no. 9, 2021, Art. no. 090547.
- [9] J. Hong, D. Lee, E. R. Jeong, and Y. Yi, "Towards the swift prediction of the remaining useful life of Lithium-Ion batteries with end-to-end deep learning," *Appl. Energy*, vol. 278, 2020, Art. no. 115646.
- [10] X. Hu, J. Jiang, D. Cao, and B. Egardt, "Battery health prognosis for electric vehicles using sample entropy and sparse Bayesian predictive modeling," *IEEE Trans. Ind. Electron.*, vol. 63, no. 4, pp. 2645–2656, Apr. 2016, doi: [10.1109/TIE.2015.2461523](https://doi.org/10.1109/TIE.2015.2461523).
- [11] K. Liu, Q. Peng, H. Sun, M. Fei, H. Ma, and T. Hu, "A transferred recurrent neural network for battery calendar health prognostics of energy-transportation systems," *IEEE Trans. Ind. Inform.*, to be published, doi: [10.1109/TII.2022.3145573](https://doi.org/10.1109/TII.2022.3145573).
- [12] K. Liu, X. Tang, R. Teodorescu, F. Gao, and J. Meng, "Future ageing trajectory prediction for Lithium-Ion battery considering the knee point effect," *IEEE Trans. Energy Convers.*, vol. 37, no. 2, pp. 1282–1291, Jun. 2022, doi: [10.1109/TEC.2021.3130600](https://doi.org/10.1109/TEC.2021.3130600).
- [13] Z. Lyu, R. Gao, and L. Chen, "Li-Ion battery state of health estimation and remaining useful life prediction through a model-data-fusion method," *IEEE Trans. Power Electron.*, vol. 36, no. 6, pp. 6228–6240, Jun. 2021, doi: [10.1109/TPEL.2020.3033297](https://doi.org/10.1109/TPEL.2020.3033297).
- [14] Y. Che, Z. Deng, X. Tang, X. Lin, X. Nie, and X. Hu, "Lifetime and aging degradation prognostics for Lithium-Ion battery packs based on a cell to pack method," *Chin. J. Mech. Eng.*, vol. 35, no. 1, pp. 1–6, 2022, doi: [10.1186/s10033-021-00668-y](https://doi.org/10.1186/s10033-021-00668-y).
- [15] J. Meng et al., "An automatic weak learner formulation for Lithium-Ion battery state of health estimation," *IEEE Trans. Ind. Electron.*, vol. 69, no. 3, pp. 2659–2668, Mar. 2022, doi: [10.1109/TIE.2021.3065594](https://doi.org/10.1109/TIE.2021.3065594).
- [16] J. Wei, G. Dong, and Z. Chen, "Remaining useful life prediction and state of health diagnosis for Lithium-Ion batteries using particle filter and support vector regression," *IEEE Trans. Ind. Electron.*, vol. 65, no. 7, pp. 5634–5643, Jul. 2018, doi: [10.1109/TIE.2017.2782224](https://doi.org/10.1109/TIE.2017.2782224).
- [17] S. Greenbank and D. Howey, "Automated feature extraction and selection for data-driven models of rapid battery capacity fade and end of life," *IEEE Trans. Ind. Inform.*, vol. 18, no. 5, pp. 2965–2973, May 2022, doi: [10.1109/TII.2021.3106593](https://doi.org/10.1109/TII.2021.3106593).
- [18] G. Dong, W. Han, and Y. Wang, "Dynamic bayesian network-based Lithium-Ion battery health prognosis for electric vehicles," *IEEE Trans. Ind. Electron.*, vol. 68, no. 11, pp. 10949–10958, Nov. 2021, doi: [10.1109/TIE.2020.3034855](https://doi.org/10.1109/TIE.2020.3034855).
- [19] Y. Che et al., "State of health prognostics for series battery packs: A universal deep learning method," *Energy*, vol. 238, 2022, Art. no. 121857.
- [20] L. Ren, J. Dong, X. Wang, Z. Meng, L. Zhao, and M. J. Deen, "A data-driven auto-CNN-LSTM prediction model for Lithium-Ion battery remaining useful life," *IEEE Trans. Ind. Inform.*, vol. 17, no. 5, pp. 3478–3487, May 2021, doi: [10.1109/TII.2020.3008223](https://doi.org/10.1109/TII.2020.3008223).
- [21] X. Zhang, Y. Qin, C. Yuen, L. Jayasinghe, and X. Liu, "Time-series regeneration with convolutional recurrent generative adversarial network for remaining useful life estimation," *IEEE Trans. Ind. Inform.*, vol. 17, no. 10, pp. 6820–6831, Oct. 2021, doi: [10.1109/TII.2020.3046036](https://doi.org/10.1109/TII.2020.3046036).
- [22] Y. Che, Z. Deng, X. Lin, X. Hu, and L. Hu, "Predictive battery health management with transfer learning and online model correction," *IEEE Trans. Veh. Technol.*, vol. 70, no. 2, pp. 1269–1277, Feb. 2021.
- [23] J. Ma et al., "Cycle life test optimization for different Li-Ion power battery formulations using a hybrid remaining-useful-life prediction method," *Appl. Energy*, vol. 262, 2020, Art. no. 114490.
- [24] X. Hu, Y. Che, X. Lin, and S. Onori, "Battery health prediction using fusion-based feature selection and machine learning," *IEEE Trans. Transp. Electrification*, vol. 7, no. 2, pp. 382–398, Jun. 2021, doi: [10.1109/TTE.2020.3017090](https://doi.org/10.1109/TTE.2020.3017090).
- [25] K. A. Severson et al., "Data-driven prediction of battery cycle life before capacity degradation," *Nat. Energy*, vol. 4, no. 5, pp. 383–391, 2019.
- [26] P. M. Attia et al., "Closed-loop optimization of fast-charging protocols for batteries with machine learning," *Nature*, vol. 578, no. 7795, pp. 397–402, 2020.
- [27] T. Baumhöfer, M. Brühl, S. Rothgang, and D. U. Sauer, "Production caused variation in capacity aging trend and correlation to initial cell performance," *J. Power Sources*, vol. 247, pp. 332–338, 2014.
- [28] E. Chemali, P. J. Kollmeyer, M. Preindl, R. Ahmed, and A. Emadi, "Long short-term memory networks for accurate state-of-charge estimation of Li-Ion batteries," *IEEE Trans. Ind. Electron.*, vol. 65, no. 8, pp. 6730–6739, Aug. 2018, doi: [10.1109/TIE.2017.2787586](https://doi.org/10.1109/TIE.2017.2787586).
- [29] H. Yao, D. lai Zhu, B. Jiang, and P. Yu, "Negative log likelihood ratio loss for deep neural network classification," *Adv. Intell. Syst. Comput.*, vol. 1069, pp. 276–282, 2020.



Yunhong Che received the B.E. and M.S. degrees in automotive engineering from College of Mechanical and Vehicle Engineering, Chongqing University, Chongqing, China, in 2019 and 2021, respectively. He is currently working toward the Ph.D. degree in power electronics with Department of Energy, Aalborg University, Aalborg, Denmark.

His research interests include modeling and state estimation, health prognostic, and lifetime prediction for lithium-ion batteries.



Daniel-Ioan Stroe (Member, IEEE) received the Dipl.-Ing. degree in automatics from the Transilvania University of Brasov, Romania, in 2008, the M.Sc. degree in wind power systems and the Ph.D. degree in lifetime modeling of Lithium-ion batteries from Aalborg University (AAU), Aalborg, Denmark, in 2010 and 2014, respectively.

He has been with AAU, since 2010. He is currently an Associate Professor with AAU Energy, where he leads the Batteries Research Group, and the Battery Systems Testing Laboratory. He was a Visiting Researcher with RWTH Aachen, Germany, in 2013. He has coauthored more than 150 journals and conference papers in various battery-related topics. His current research interests include the area of energy storage systems for grid and e-mobility, Lithium-based batteries testing, modelling, and diagnostics and their lifetime estimation.



Xiaosong Hu (Senior Member, IEEE) received the Ph.D. degree in automotive engineering from the Beijing Institute of Technology, Beijing, China, in 2012. He did scientific research and the Ph.D. dissertation with the Automotive Research Center, University of Michigan, Ann Arbor, MI, USA, between 2010 and 2012.

He is currently a Professor with the Department of Mechanical and Vehicle Engineering, Chongqing University, Chongqing, China. He was a Postdoctoral Researcher with the Department of Civil and Environmental Engineering, University of California, Berkeley, CA, USA, between 2014 and 2015, as well as at the Swedish Hybrid Vehicle Center and the Department of Signals and Systems at Chalmers University of Technology, Gothenburg, Sweden, between 2012 and 2014. He was also a Visiting Postdoctoral Researcher with the Institute for Dynamic Systems and Control, Swiss Federal Institute of Technology, Zurich, Switzerland, in 2014. His research interests include modeling and control of alternative powertrains and energy storage systems.



Remus Teodorescu (Fellow, IEEE) received the Dipl.Ing. degree in electrical engineering from the Polytechnical University of Bucharest, Bucharest, Romania, in 1989, and the Ph.D. degree in power electronics from the University of Galati, Romania, in 1994.

In 1998, he was with the Department of Energy Technology, Aalborg University, Aalborg, Denmark, where he is currently a Full Professor. Between 2013 and 2017, he has been a Visiting Professor with Chalmers University. He is IEEE/PELS Fellow since 2012 for contributions to grid converters technology for renewable energy systems.

In 2022, he was a Villum Investigator and the leader of Center of Research for Smart Battery, Aalborg University. His main current research include li-ion battery state estimation and prediction with AI and smart batteries, and modular multilevel converters for HVDC/FACTS.